Annual Review of Marine Science

Global Air-Sea Fluxes of Heat, Freshwater, and Momentum: Energy Budget Closure and Unanswered Questions

Lisan Yu

Department of Physical Oceanography, Woods Hole Oceanographic Institution, Woods Hole, Massachusetts 02543, USA; email: lyu@whoi.edu

Keywords

global-ocean energy budget, global-ocean freshwater budget, air–sea heat flux, air–sea freshwater flux, wind stress, air–sea buoy measurements, atmospheric reanalysis, satellite observations

Abstract

The ocean interacts with the atmosphere via interfacial exchanges of momentum, heat (via radiation and convection), and fresh water (via evaporation and precipitation). These fluxes, or exchanges, constitute the oceansurface energy and water budgets and define the ocean's role in Earth's climate and its variability on both short and long timescales. However, direct flux measurements are available only at limited locations. Air–sea fluxes are commonly estimated from bulk flux parameterization using flux-related near-surface meteorological variables (winds, sea and air temperatures, and humidity) that are available from buoys, ships, satellite remote sensing, numerical weather prediction models, and/or a combination of any of these sources. Uncertainties in parameterization-based flux estimates are large, and when they are integrated over the ocean basins, they cause a large imbalance in the global-ocean budgets. Despite the significant progress that has been made in quantifying surface fluxes in the past 30 years, achieving a global closure of ocean-surface energy and water budgets remains a challenge for flux products constructed from all data sources. This review provides a personal perspective on three questions: First, to what extent can time-series measurements from air–sea buoys be used as benchmarks for accuracy and reliability in the context of the budget closures? Second, what is the dominant source of uncertainties for surface flux products, the flux-related variables or the bulk flux algorithms? And third, given the coupling between the energy and water cycles, precipitation and surface radiation can act as twin budget constraints—are the community-standard precipitation and surface radiation products pairwise compatible?

1. INTRODUCTION

The ocean's role in climate is manifested in its ability to transport heat poleward and regulate climate variability through exchange of heat, fresh water, and momentum with the atmosphere (e.g., Trenberth & Caron 2001, Wunsch 2005, Stephens et al. 2012, Wild et al. 2013). The fluxes, or exchange, at the air–sea interface are fundamental processes for keeping the global climate system in balance with the incoming insolation at Earth's surface (Loeb et al. 2012, Trenberth et al. 2014). They are also a primary conduit for coupling and feedback between the ocean and atmosphere on a broad range of scales, from synoptic weather events to regional and global circulation systems (e.g., Drennan et al. 2007, Føre et al. 2012, Gulev & Belyaev 2012, Drijfhout et al. 2014, Soloviev et al. 2014). Uncertainties in air–sea fluxes challenge our ability to understand how the ocean interacts with the atmosphere to influence the climate patterns worldwide, and how the interaction can be represented in Earth system models to improve the prediction of extreme weather events at long lead times. Air–sea flux products with not only high quality but also continuous and consistent climate records are sought to serve the needs of ocean and climate communities for the characterization, attribution, and modeling of weather and climate variability in the atmosphere and ocean (e.g., WGASF 2000, Curry et al. 2004, Fairall et al. 2010, Gulev et al. 2010).

Significant progress has been made in the past four decades in understanding and measuring the turbulent motions near the air–sea boundary (e.g., breaking waves, turbulence, sea spray, rain, and surface films) and their cumulative effects on the rates of transports of heat,moisture, and momentum across the interface (e.g., Louis 1979, Large&Pond 1981, Andreas et al. 1995, DeCosmo et al. 1996, Edson et al. 1998, Grachev et al. 2003, Weller et al. 2008). The direct covariance (or eddy correlation) technique (Crawford et al. 1993) has so far been the only established means for direct flux measurements at sea (e.g., Edson et al. 1998, Landwehr et al. 2015). However, direct flux measurements are currently available only at a limited number of locations for limited durations, because the measurements of vertical winds as well as temperature and humidity fluctuations need to be conducted on specially designed ships or buoys to minimize the effects of flow distortion and turbulent injection induced by the moving platforms. Air–sea fluxes in numerical models and global data products are computed from flux parameterizations that link the microscale turbulent transfers to easily measured macroscale quantities such as near-surface wind, humidity, and temperature. Sophisticated parameterizations have been developed, including the inertial-dissipation method, which infers surface fluxes from spectral characteristics of the inertial subrange (Fairall & Larsen 1986); the mean flux-profile method, which utilizes the empirical relationships between surface fluxes and mean profiles (gradients) of observed quantities in the surface layer (Paulson et al. 1972, Blanc 1983); and the bulk aerodynamic method, which employs the Monin–Obukhov similarity theory (Monin&Obukhov 1954, Garratt 1977, Large&Pond 1981). The bulk approach provides scaling relationships between surface fluxes and profiles of mean variables in the surface layer, and it determines the transfer coefficients from either empirically derived flux profiles (Liu et al. 1979) or direct covariance experiments (Fairall et al. 1996, 2003; Edson et al. 2013).

Of all types of parameterizations, the bulk aerodynamic parameterization is and will continue to be significant for air–sea flux estimation due to its easy applicability. The required input information of near-surface meteorology is routinely available from voluntary observing ships (VOSs), satellite remote sensing, and numerical weather prediction models. The algorithm developed during the Tropical Ocean–Global Atmosphere (TOGA) Coupled Ocean–Atmosphere Response Experiment (COARE) (Fairall et al. 1996, 2003; Edson et al. 2013) represents the state of the art in accuracy (Brunke et al. 2003) and has been used widely in constructing global air–sea flux gridded products using satellite and ship observations.

Using bulk parameterization, one can approximate surface turbulent momentum, heat, and freshwater fluxes as

$$\tau_x = \rho c_d u(U - U_s) \quad (1)$$

$$\tau_y = \rho c_d v(U - U_s) \quad (2)$$

$$LH = \rho L_v c_e (U - U_s)(q_s - q_a) \quad (3)$$

$$SH = \rho c_p c_h (U - U_s)(T_s - T_a) \quad (4)$$

$$E = LH/\rho_w L_v \quad (5)$$

where τ_x and τ_y are the respective zonal and meridional wind stress components, *LH* the latent heat flux, *SH* the sensible heat flux, and *E* the moisture flux. The input variables for calculating the fluxes (1)-(5) are the zonal (u), meridional wind (v) components, and wind speed (U) at a reference height, the ocean-surface current velocity (U_s) that is usually small, sea-surface temperature (SST, T_s), the potential air temperature (T_a) and specific humidity (q_a) at a reference height, and saturation specific humidity (q_s) as a function of T_s and sea level pressure. The other constants are ρ the air density, ρ_w the sea-water density, L_v the latent heat of vaporization that is expressed as $L_e = (2.501 - 0.00237 \times T_s) \times 1.0^6$, and c_p the isobaric specific heat. The turbulent transfer coefficients, c_d, c_e, and c_h, depend on wind speed, atmospheric stability, measurement height, surface roughness, surface wave height, and wave age (e.g., Charnock 1955; Drennan et al. 2003; Andreas et al., 2008; Edson et al. 2013). Bulk flux algorithms differ from each other mainly in how roughness length is parameterized under various wind speeds. Significant uncertainties in these coefficients still remain (Zeng et al. 1998; Brunke et al. 2002), particularly under very weak wind ($U < 4$ ms^{-1}) (e.g. Chang and Grossman 2007) or storm force ($U > 24$ ms^{-1}) conditions (e.g. Powell et al. 2003; Andreas et al. 2008).

Air–sea exchange at the ocean surface comes not only in the form of turbulent fluxes by evaporation (LH) and conduction (SH) but also by means of radiative fluxes by shortwave and longwave radiation. Evaporation releases not only latent heat but also water vapor (see Eqs. (3) and (5)). Because of the large amount of latent heat exchange during phase change to liquid water (approximately 2.5×10^6 J kg^{-1} if SST effect is small), the transport of water vapor is regarded as the energy transport. Therefore, the water cycle is closely linked to the energy cycle, with the atmospheric circulation acting as the linchpin connecting the atmosphere and the ocean. The energy (hereafter denoted by Q_{net}) and freshwater (hereafter FW) budgets over the global ocean surface are expressed as:

$$Q_{net} = SW - LW - LH - SH \qquad (6)$$

$$FW = P - E + R \qquad (7)$$

where SW is the net downward shortwave radiation, LW the net upward longwave radiation, P the precipitation, and R the river runoff. Energy and water budgets are conserved quantities, and so Q_{net} and FW must be close to zero when integrated over the global ocean on annual and long-term mean basis. However, all parameterization-based flux products, constructed from either ship reports or satellite observations, do not include the ice-covered Polar Regions due to the lack of reliable observations. In this regard, the globally averaged mean represents a mean over the global ice-free open ocean rather than the entire global ocean, and so, the long-term mean average of Q_{net} should not be closed exactly zero but within 2 – 3 Wm^{-2} (Serreze et al. 2007; Bengtsson et al. 2013).

The ability to close the energy and freshwater budgets at the ocean surface has become a test of the accuracy of gridded flux products (Isemer et al 1989; Josey et al 1999; Fairall et al. 2010; Gulev et al. 2010; Yu et al. 2013; Von Schuckmann et al. 2016; Liu et al. 2017; Valdivieso et al. 2017). This review is to provide an integrative view of leading issues that challenge the parameterization-based flux products in achieving the energy and freshwater budget closures.

2. Energy and Freshwater Budget Closures and Leading Issues

2.1 Leading issues

Flux products are known to have large uncertainties that stem from both the uncertainties in flux-related variables (u, v, U, q_a, T_a, and T_s) and the uncertainties in estimates of transfer coefficients (c_d, c_e, and c_h) in the bulk flux algorithms (Isemer et al. 1989; Josey et al. 1999; Brunk et al. 2003; Valdivieso et al. 2017). Satellite observations represent major improvements over VOS observations owing to their unprecedented sampling frequencies, spatial resolution, and truly global coverage. Nonetheless, space-borne sensors cannot resolve the thermal quantities, T_a and q_a, at a few meters above the surface, because the measured radiation is emitted from relatively thick atmospheric layers rather than from single levels (Simonot and

Gautier, 1989; Schulz et al. 1993). A common approach is to retrieve T_a and q_a from satellite observed total column-integrated water vapor using in situ measurements as reference (Liu 1988; Schlüssel et al 1995), but the empirically-based retrieval algorithm may overly simplify the dependence of the vertical distribution of water vapor content on atmospheric stability and the advection of the large-scale circulation (Esbensen et al. 1993). There are substantial biases in T_a and q_a retrievals that are regime dependent (Yu and Jin 2018), and these biases have been the leading source of error for satellite-based flux products (Curry et al. 2004; Jackson et al. 2006; Prytherch et al. 2015).

The accuracy requirement for Q_{net} is 10 Wm^{-2} for flux application on monthly-to-seasonal timescales (WCRP 1989; Webster and Lukas 1992; WGASF, 2000; Weller et al. 2004; Bradley and Fairall, 2007). If the goal is to detect long-term trends from a background of natural variability, the accuracy requirement is at least one order of magnitude higher, at O(1 W m^{-2}) for Q_{net} and O(1 cm yr^{-1}) for FW (Hansen et al. 2005; Levitus et al. 2005). Parameterization-based flux products all have difficulty closing the ocean heat budget within the above limits. Ship-based climatological analyses show mean heat gains of ~ 30 W m^{-2} or greater by the ocean (Isemer et al. 1989; Large et al. 1997; Josey et al. 1999), and satellite-based products have a similar degree of imbalance (Liu et al. 2017). Some assumed that the imbalance is caused by errors in various flux formulae, which can be corrected by proportional adjustment of the flux components (Isemer et al. 1989; da Silva et al. 1995; Large and Yeager 2009), while some suggested that the significant source of error may come from various regional biases in flux-related variables. These biases may arise from the undersampling of extreme conditions in regions such as the high latitudes and the western boundary currents (Josey et al. 1999), uncorrected biases in T_a and q_a (Jin et al. 2015), etc. Hence, the unbalanced flux products are often adjusted by using inverse analysis (Isemer et al. 1989) with hydrographic heat transport constraints to close the global-ocean energy budget (Grist and Josey 2003). More recently, attempts are made to determine an unbiased Q_{net} from combining satellite-based net radiation at the top of the atmosphere (Rad_{TOA}) and the divergence of vertically integrated horizontal atmospheric energy transports, using the global mean Rad_{TOA} from the Clouds and the Earth's Radiant Energy System–Energy Balanced and Filled product (CERES-EBAF; Loeb et al. 2009) that is anchored to estimates of global mean ocean heat storage.

Despite much progress since the work by Isemer et al. (1989) and Josey et al. (1999), the inability to close the ocean heat budget remains a common problem in present parameterization-based products that are largely constructed from satellite observations. Among a number of fundamental issues that are yet to be answered, the following three are most critical. First, all flux products have been rested on the assumption that a good comparison with high-quality independent measurements from air-sea buoys warrants accuracy and reliability. Then, why can't the energy budget be closed even though flux products are in good agreement with buoy measurements? Second, there seems to be a consensus that the primary source of the energy budget imbalance is the underestimation of *LH* by about 15%, using the inverse flux adjustment analysis (Isemer et al. 1989; Grist and Josey 2003) and the vertically integrated energy budget adjustment (Liu et al. 2017). Is the underestimation caused solely by biases in flux-related variables (such as q_a)? Or does the bulk flux parameterization also play a role? Thirdly, the ocean energy and freshwater budgets are connected through *LH* (Eqs. (6)-(7)), suggesting that the amount by which *LH* needs to be adjusted to close the energy budget can potentially be constrained using the ocean freshwater budget. Nowadays the surface radiation product from CERES-EBAF (Kato et al. 2013; Loeb et al. 2018) and the precipitation product from the Global

Precipitation Climatology Project (GPCP**)** (Adler et al. 2003) have become community standard products. Can they be paired to help diagnose the leading sources of uncertainties in parameterization-based turbulent flux products? The three issues are reviewed below.

2.2 Flux products

Different products use different bulk formulae. Satellite-derived flux products (e.g., Chou et al. 1995; Kubota et al. 2002; Roberts et al. 2010; Andersson et al. 2011; Bentamy et al. 2013; Yu and Jin 2014;2018) are all established from the COARE bulk flux algorithms (Fairall et al. 1996; 2003; Edson et al. 2013). The ship-based turbulent flux climatology compiled by the National Oceanographic Centre (NOC) (Josey et al., 1999; Berry and Kent 2011) is computed from Smith (1988) algorithm. Atmospheric reanalyses have their own bulk parameterization schemes (Kalnay et al. 1996; Kanamitsu et al. Saha et al. 2010; Dee et al, 2011; Rienecker et al. 2011; Kobayashi et al. 2015; Molod et al., 2015). Surface flux products differ from each other because input data sources (satellite, VOS reports, and NWP models) have uncertainties arising from at least one of the deficiencies: incomplete global coverage, indirect satellite retrievals, systematic bias, and random error. Surface flux products are also sensitive to the choice of algorithms (e.g., Webster and Lukas 1992; Miller et al. 1992; Zeng et al. 1998; Brunke et al. 2003).

The Objectively Analyzed air–sea Fluxes (OAFlux) project at the Woods Hole Oceanographic Institution (WHOI) has been through two phases of flux product development. The first phase led to a 1°-gridded turbulent heat and moisture (i.e. *LH*, *SH*, and *E*) flux analysis (hereafter OAFlux-1x1), with q_a and T_a determined from objective synthesis of satellite-derived retrievals and atmospheric reanalyses and *U* from multiple satellite sensors (Yu and Weller 2007;

Yu et al. 2008). The second phase of development has focused on constructing high-resolution (HR; 0.25°-gridded), full-range (i.e., *LH, SH, E,* τ_x and τ_y) turbulent flux products (hereafter OAFlux-HR), with flux-related variables determined solely from satellite retrievals (Jin and Yu 2013; Yu and Jin 2014; 2018). Compared to OAFlux current 1°-gridded analysis (hereafter OAFlux-1x1; Yu and Weller 2007; Yu et al. 2008), OAFlux-HR has made improvements in three main aspects: spatial resolution, q_a and T_a estimates, and the inclusion of momentum fluxes. The improvement leads to an increase of LH+SH by ~ 8 Wm^{-2}, but disappointingly, it does not lead to an energy budget closure. When combined with CERES EBAF surface radiation (SW-LW), OAFlux-1x1 LH+SH produces a mean heat gain of ~ 25 Wm^{-2} over the global ocean while OAFlux-HR LH+SH has a gain of ~ 17 Wm^{-2}. Since CERES EBAF has been adjusted to balance the Earth's energy budget, the imbalance is once again pointed to as-yet uncorrected bias in OAFlux-HR. From the viewpoint of the flux variable estimation, the argument is not convincing. The OAFlux-HR satellite-derived variables, q_a, T_a, and U, have thoroughly validated with in situ time series measurements at more than 120 locations. The mean biases relative to buoy measurements are – 0.34 g kg^{-1} for q_a (i.e. a dry bias), – 0.08ºC for T_a (i.e., a slight cold bias), and – 0.13 m s^{-1} for U (i.e., a weak bias) (Yu and Jin 2012; 2018). A simple error diagnosis of the bulk formula for LH and SH, assuming a mean wind speed of 7 m s^{-1}, suggests that the adjustment of 17 W m^{-2} imbalance requires the mean state of the near-surface air to be either further dried up by 0.74 g kg^{-1} or cooled down by 0.46ºC. The magnitude of adjustment is way beyond the product accuracy defined by buoy evaluation.

Uncertainty in bulk flux algorithm is the only stone left unturned in our pursuit of surface energy budget closure. When comparing the two versions of OAFlux products with atmospheric reanalyses, the influence of bulk algorithms on surface flux estimates is evident. Hence, there is a need for understanding the uncertainties in both flux-related variables and bulk algorithms to gain a complete understanding of the cause of surface budget imbalance, Since satellite-derived products are all produced from COARE version 3 (v3), differences between products reflect the differences between variable estimation which have been characterized by several comparison studies (Betamy et al. 2017). To narrow down the scope of this review, we limit the discussion to 9 atmospheric reanalyses, 2 OAFlux products, and the ship-based NOC, and use CERES and GPCP as budget constraints (Table 1).

The OAFlux-HR full-range turbulent flux products can be combined with CERES and GPCP to provide a complete description of ocean-surface heat, freshwater, and momentum fluxes. The annual-mean fields of Q_{net} from CERES and OAFlux-HR, *E-P* from OAFlux-HR and GPCP, and wind stress vector and wind stress curl (i.e. $\partial\tau_y/\partial x - \partial\tau_x/\partial y$) from OAFlux-HR in 2014 (Figure 1). Consistent with the climatological mean patterns (e.g. Josey et al. 2013), the tropical ocean is the primary region of atmospheric heat and freshwater input to the ocean and the subtropical ocean, particularly the western boundary current (WBC) regime, is the region of oceanic heat and freshwater transfer to the atmosphere. In the Northern Hemisphere, cyclonic (positive) wind stress curl drives an upward Ekman pumping and upwelling, while anticyclonic (negative) wind stress curl drives Ekman suction and downwelling. In the Southern Hemisphere, the effects are opposite with cyclonic (positive) wind stress curl denoting downwelling and anticyclonic (negative) wind stress curl upwelling. Although CERES SW and LW are 1° gridded and GPCP precipitation 2.5° gridded, the high-resolution advantage of OAFlux-HR in depicting the fine structure of frontal-scale air-sea exchanges is seen in the WBC regimes.

2.3 Differences in bulk parameterization algorithms

Unlike OAFlux-1x1 that is constructed from COARE v3, the OAFlux-HR flux fields in Figure 1 are computed from an updated COARE bulk flux algorithm, version 4 (Edson et al. 2010; 2012; 2013). COARE v4 (Jim Edson, personal communication) has focused on improving turbulent transfer coefficients, particularly, c_e and c_h for *LH* and *SH*. In COARE v3, the coefficients for *LH* and *SH* are identical, assuming similarity in the transfer of heat and mass. In COARE v4, *LH* and *SH* are modeled with separate formulae and validated with direct flux measurements from field programs. The c_e estimate in the two algorithms exhibits the same overall characteristics of a minimum around wind speed at 3 – 4 ms^{-1}; after that, c_e in COARE v4 increases to a maximum around wind speed at 12 ms^{-1} before falling off at higher winds, while c_e in COARE v3 shows a near-linear increase with wind speed. In the following, OAFlux-HR computed from COARE v3 is denoted OAFlux-HR3 and that from COARE v4 is OAFlux-HR4.

The zonal averages of the annual-mean LH+SH fields in 2014 from OAFlux-HR3, -HR4, and OAFlux-1x1 and their differences (Figures 2a-b) show that the three products differ most at low and mid latitudes. The differences between OAFlux-HR3 and -HR4 reflect the change induced by COARE algorithms, and v4 produces stronger LH+SH at all latitudes with maximum differences of ~20 Wm^{-2} at 30–40° latitudes north and south. The latter are the locations of strong turbulent heat loss associated with WBCs. The differences between OAFlux-1x1 and -HR3 reflect the change made in flux variables due to resolution change and the use of satellite-only input data source, and the improvement leads to an averaged increase of ~10 Wm^{-2} for the latitudes between 40°S and 40°N. In general, COARE v3 is a weaker algorithm compared to v4.

To assess the difference between COARE v3 and the bulk flux algorithms in reanalyses, the flux-related variables from NCEP1, CFSR, ERA-interim, and MERRA were used as input to COARE v3 to compute a set of COARE v3-based reanalysis fluxes. The zonally averaged mean differences between the original reanalysis fluxes and the COARE v3-based reanalysis fluxes in 2014 (Figures 2c-d) indicate that COARE v3 is a weak algorithm compared to the four reanalysis algorithms. The ERA-interim algorithm is the closest to COARE v3, and the differences are mostly within 5 Wm^{-2} except for a 10 Wm^{-2} spike at ~15°N/S. The NCEP1 algorithm has the largest departure from COARE v3, with magnitude approaching 40 Wm^{-2} at subtropical latitudes. CFSR and MERRA algorithms are respectively about 8 and 12 Wm^{-2} stronger at most latitudes.

2.4 Interpretation of buoy evaluation

Time series measurements from moored air-sea buoys in the global ocean serve as benchmarks for validating flux products constructed from various sources (Fairall et al. 2010; Gulev et al. 2010; Yu et al. 2013; Bentamy et al. 2017; Valdivieso et al. 2017). Despite good comparisons, none of flux products is yet able to achieve an energy budget closure if additional adjustments are not imposed (e.g. Isemer 1989; Josey et al. 1999). Two factors might be responsible for this. One is that buoy fluxes are not measured but computed (Weller et al. 2008), and the algorithm for buoy LH+SH is COARE v3. The computed buoy fluxes may not be bias free if there is uncertainty in the flux algorithm (Figure 2). The other is that the majority of buoys are deployed in the tropical warm water zone with very limited number of buoys in the vicinity of WBCs and high-latitude cold water zone (Figure 3a).

To illustrate that COARE v3-based buoy fluxes may not be a viable verification for flux products, we computed daily-mean buoy fluxes (in terms of SW-LW and LH+SH) that were acquired between 1990 and 2015 at 126 buoy locations (Figure 3a) and compared with collocated daily-mean CERES SW-LW, OAFlux-1x1 LH+SH and 6 atmospheric reanalyses (SW-LW and LH+SH). Since surface fluxes are a sensitive function of SST, we binned the product-minus-buoy flux differences onto every 0.5°C SST grids using buoy observations. Distribution of product-minus-buoy differences with SST (Figures 3b-c) indicates that there are some exceptionally large values in a few SST regimes: low SSTs (<6°C), SSTs of 15-20°C, and very high SSTs (>30°C). The number of available buoy measurements is limited (less than 50) in these SST ranges so that the performance of flux products may not be statistically well represented. Away from these ranges, the errors in reanalysis SW-LW increase sharply for SST greater than 20°C, which corresponds to the tropical-subtropical warm water regime. Only satellite-derived CERES SW-LW is unbiased. As for error distribution in LH+SH, all reanalyses have a similar error distribution pattern: errors are smaller when SST is less than 15°C and larger when SST is greater than 20°C. Except for NCEP1 and MERRA, the errors remain more or less constant for SST between 20 – 28°C though with varying magnitude. JRA55 differs by more than 40 Wm^{-2}, ERA-interim by 20 Wm^{-2}, and CFSR by 17 Wm^{-2}. OAFlux-1x1 is largely unbiased - but it is computed from COARE v3, the same algorithm used by buoy fluxes. Given COARE v3 is weak in comparison with reanalysis algorithms (Figures 2c-d), it is yet to be determined which is a more dominant source of uncertainty for LH+SH products, the bulk algorithm or the flux-related variables.

2.5 Differences in long-term mean fields

The standard deviations (STD) between 12 mean Q_{net} products (Table 1) averaged over the overlapping 10-year period of 2000-2010 conveys the same message that surface heat flux estimates are most uncertain in the tropical and subtropical region (Figure 4a). In the Indo-Pacific warm pool, for instance, the STD differences between products exceed 30 Wm^{-2}, which are greater than the ensemble mean of the products. Zonal averages of the 10-year mean Q_{net}, SW-LW, and LH+SH (Figures 4b-d) indicate that JRA55 Q_{net} is an outliner, as its LH+SH is excessively strong in the tropics. OAFlux-HR4 is in the same range as reanalysis LH+SH between 25-45°N/S, but is stronger than the reanalysis at mid latitudes because the high resolution of HR4 can better resolve the LH+SH associated with the WBC fronts.

The STD differences between 11 mean *E-P* products averaged over 2001-2010 (Figures 5a-c) are most pronounced in the tropical/subtropical regions between 30°S and 30°N. Major uncertainty is the spread in *P* products in regions of the Intertropical Convergence Zone (ITCZ) and South Pacific Convergence Zone (SPCZ), with the satellite-based GPCP having the weakest rainfall and JRA55 the strongest rainfall. The pattern of differences suggests that reanalyses have difficulty in simulating tropical convective clouds and rainfall processes (Rosenfeld and Lensky 1998; Newman et al. 2000; Yu et al. 2017). In contrast to the STD *E-P* pattern, the STD differences between 11 mean wind stress magnitude, τ, products averaged over 2001-2010 show that large deviations are located at mid to high latitudes where winds are strong (Figure 6a). The zonal averages reveal that the spread in the products is caused primarily by the gaps between two groups, the group that assimilates satellite scatterometers (i.e. CFSR, ERA-interim, JRA55, MERRA, and MERR2, OAFlux-HR) and the group that does not (NCEP2, ERA20C, and 20CR). Winds are vectors, which explain that the zonal averages of τ_x and τ_y are not proportional to the zonal average of τ due to the sign cancellation (Figures 6b-c).

2.6 Surface budget imbalance: are CERES and GPCP compatible constraints?

Given the large uncertainties in surface flux estimates in the tropical-subtropical ocean, it is not a surprise that the surface energy and freshwater budgets determined by the mean Q_{net} and *E-P* products differ considerably between them. (Figures 7a-b). The surface energy budget ranges from a significant ocean heat deficit of -16 W m^{-2} by JRA55 to a significant ocean heat gain of 25 Wm^{-2} by OAFlux-1x1. The surface freshwater budget ranges from a nearly perfect balance between *E* and *P* by CFSR to a large freshwater imbalance of 27 cm yr^{-1} by the combined OAFlux-HR4 and GPCP. Interestingly, the product series of OAFlux affects the surface energy and freshwater budget balance in an opposite way. While the imbalance in the energy budget is reduced by the order from OAFlux-1x1, to HR3, and to HR4, the imbalance in the freshwater budget is increased in the same order.

The scatter plots between *SW-LW* and *LH+SH* and between *E* and *P* (Figures 7c-d) shed some light on how the ocean and atmospheric flux components could be partitioned to achieve balanced budgets. As stated in the Introduction, the energy budget determined from surface heat flux products is expected to achieve a closure within 2 – 3 Wm^{-2} due to the exclusion of Polar regions. This implies that *SW-LW* should be balanced with *LH+SH* within the limit. Surface radiative budgets from CERES, NOC, ERA-interim, and CFSR agree well with each other, but the deviations in LH+SH set the total budgets apart. OAFlux-HR4 is a far better match for CERES compared to OAFlux-1x1. However, this works opposite for the freshwater budget. On the long-term mean basis, the ocean freshwater budget should be balanced, that is $E - P - R \approx 0$ (Eq.(7)). If expressing the *E/P* in terms of $E/P \approx (P+R)/P = 1 + R/P$, one can expect that the larger (smaller) the ratio, the more (less) continental runoff is needed to balance the water budget over the ocean. The *E/P* ratio is found to be about 1.1 in most reanalysis products (Yu et al. 2017). OAFlux-1x1and GPCP fall exactly on the line that delineates $E/P = 1.1$ (Figure 7d), while HR4 is significantly off.

CERES EBAF and GPCP are community standard products. The improvement made in OAFlux-HR4 improves the surface energy budget constrained by CERES but deteriorates the surface freshwater budget constrained by GPCP. Looking at the scatter relationships (Figures 7c-d), CERES surface heat input is on the higher end and consistent with three reanalyses. By comparison, GPCP freshwater input is lowest among all reanalyses. Are GPCP and CERES pairwise compatible in terms of surface energy and freshwater budgets?

3. FUTURE PERSPECTIVES

This review presents a perspective on the imbalance in surface energy and freshwater budgets using parameterization-based flux products. Most viewpoints stem from our own decade-long research developing surface turbulent heart, moisture, and momentum fluxes from satellite observations. The inability to close the surface energy budget, despite many efforts that have been made to improve the estimates of flux-related variables, has led us to reframe our thinking and embrace questions that are still largely unanswered. Achieving globally balanced energy and freshwater budgets is a multifaceted challenge, and this review has focused on only three questions. Nonetheless, our study stresses the importance of collaborations between various groups to understand and resolve a number of discrepancies in the present-day turbulent flux estimates. These include the differences between COARE algorithms and bulk flux parameterizations used in atmospheric reanalyses, differences in flux-related variables from VOS reports, satellite observations, and atmospheric reanalysis outputs, and differences between surface radiation and precipitation products in the context of surface energy and water cycles.

Efforts addressing the following three aspects are particularly relevant. First, in situ air–sea measurements of fluxes-related variables, though limited in space, are indispensible for establishing benchmark accuracy for gridded flux products, as well as for maintaining long-term stability. To advance the skills of bulk flux parameterizations, more direct flux measurements are needed. Second, cross-comparisons among hierarchy products from varied sources are useful in identifying and understanding the uncertainties in flux products. In this regard, atmospheric reanalyses are excellent tool for such study. Lastly, limitations in current in situ air–sea observing capability suggest the need to include ocean observations and ocean data-model syntheses to achieve greater consistency by balancing the regional and/or global energy and freshwater budgets.

DISCLOSURE STATEMEMT

The author is not aware of any affiliations, memberships, funding, or financial holdings that might be perceived as affecting the objectivity of this review.

ACKNOWLEDGEMENTS

This work was supported by funding from NOAA Ocean Observing and Monitoring Division, NOAA Climate Reanalysis Task Force Team activity, and NASA Ocean Vector Wind Science Team activity. X. Jin provided programming help. J. Edson is sincerely thanked for providing the COARE programming codes.

LITERATURE CITED

Adler, R.F., et al., 2003: The Version-2 Global Precipitation Climatology Project (GPCP) Monthly Precipitation Analysis (1979–Present). J. Hydrometeor., 4, 1147–1167

Andreas, E.L., J.B. Edson, E.C. Monahan, M. Rouault, and S.D. Smith, 1995: The spray contribution to net evaporation from the sea: A review of recent progress. Boundary- Layer Meteorol., 72, 3-52.

Andreas, E. L., P. O. G. Persson, and J. E. Hare, 2008: A bulk turbulent air-sea flux algorithm for high-wind, spray conditions. J. Phys. Oceanogr., 38, 1581-1596.

Bengtsson, L., K.I. Hodges, S. Koumoutsaris, M. Zahn, and P. Berrisford, 2013: The Changing Energy Balance of the Polar Regions in a Warmer Climate. J. Climate, 26, 3112–3129.

Bentamy, A., Grodsky, S.A., Katsaros, K.B., Mestas-Nuñez, A.M., Blanke, B., Desbiolles, F., 2013. Improvement in air–sea flux estimates derived from satellite observations. Int. J. Remote Sens. 34 (14).

Bentamy, A., et al. 2017: Review and assessment of latent and sensible heat flux accuracy over the global oceans. Remote Sensing Environ. 201, 196-218.

Berry, D. I., E.C. Kent, 2011: Air–Sea fluxes from ICOADS: the construction of a new gridded dataset with uncertainty estimates. International Journal of Climatology, 31 (7). 987-1001.10.1002/joc.2059

Blanc, T. V., 1983: An Error Analysis of Profile Flux, Stability, and Roughness Length Measurements Made in the Marine Atmospheric Surface Layer, Boundary-Layer Meteorol, 26, 243-267.

Bradley, F. and C. Fairall, 2007: A Guide to Making Climate Quality Meteorological and Flux Measurements at Sea . NOAA Technical Memorandum OAR PSD-311, NOAA/ESRL/PSD, Boulder, CO, 108 pp.

Brunke, M. A., C. W. Fairall, X. Zeng, L. Eymard, and J. A. Curry, 2003: Which bulk aerodynamic algorithms are least problematic in computing ocean surface turbulent fluxes? J. Climate, 16, 619–635.

Crawford, T. L., R. T. McMillen, T. P. Meyers, and B. B. Hicks, 1993: Spatial and temporal variability of heat, water, vapor, carbon dioxide, and momentum air-sea exchange in a coastal environment. J. Geophys. Res., 98, 12 869–12 880, doi:10.1029/ 93JD00628.

Chang, H. and R. L. Grossman, 1999: Evaluation of bulk surface flux algorithms for light wind conditions using data from the coupled ocean-atmosphere response experiment (COARE). Q.J.R. Meteorol. Soc., 125: 1551-1588.

Charnock, H., 1955: Wind stress on a water surface. Quart. J. Roy. Meteor. Soc., 81, 639–640, doi:https://doi.org/10.1002/qj.49708135027.

Chou S.-H., R. M. Atlas, C-L. Shie and J. Ardizzone, 1995: Estimates of Surface Humidity and Latent Heat Fluxes over Oceans from SSM/I Data, Mon. Wea. Rev., 123, 2405-2425.

Curry, J. A., et al., 1999: High-resolution satellite-derived dataset of the ocean surface fluxes of heat, freshwater and momentum for the TOGA COARE IOP. Bull. Amer. Meteorol. Soc., 80, 2059-2080.

DeCosmom, J., K. B. Katsaros, S.D.Smith, R.J.Anderson, W. A. Oost, K. Bumke, and H. Chadwick, 1996: Air- sea exchange of water vapor and sensible heat: The humidity exchange of the sea experiment (HEXOS) results. /. Geophys. Res., 101 (C5), 12,001-12,016.

Dee, D. P., et al., 2011: The ERA-Interim reanalysis: Configuration and performance of the data assimilation system. Quart. J. R. Meteorol. Soc., 137, 553-597, doi:10.1002/qj.828.

Drennan, W. M., J. Zhang, J. R. French, C. McCormick, and P. G. Black, 2007: Turbulent fluxes in the hurricane boundary layer. Part II: Latent heat flux. J. Atmos. Sci. 64, 1103–1115.

Drennan, W. M., H. C. Graber, D. Hauser, and C. Quentin, 2003: On the wave age dependence of wind stress over pure wind seas. J. Geophys. Res., 108, 8062, doi:https://doi.org/10.1029/2000JC000715.

Drijfhout, S. S., A. T. Blaker, S. A. Josey, A. J. G. Nurser, B. Sinha, and M. A. Balmaseda, 2014: Surface warming hiatus caused by increased heat uptake across multiple ocean basins, Geophys. Res. Lett., 41, 7868–7874, doi:10.1002/2014GL061456.

Edson, J.B., A.A. Hinton, K.E. Prada, J.E. Hare, and C.W. Fairall, 1998: Direct Covariance Flux Estimates from Mobile Platforms at Sea. J. Atmos. Oceanic Technol., 15, 547–562.

Edson, J.B., V. Jampana, R.A. Weller, S.P. Bigorre, A.J. Plueddemann, C.W. Fairall, S.D. Miller, L. Mahrt, D. Vickers, and H. Hersbach, 2013: On the Exchange of Momentum over the Open Ocean. J. Phys. Oceanogr., 43, 1589–1610.

Esbensen, S. K., D. B. Chelton, D. Vockers, and J. Sun, 1993: An analysis of errors in Special Sensor Microwave Imager evapo- ration estimates over the global oceans. J. Geophys. Res., 98, 7081–7101

Fairall, C. W. and S. E. Larsen, 1986: Inertial Dissipation Methods and Turbulent Fluxes at the Air Ocean Interface, Boundary-Layer Meteorol. 34, 287-301.

Fairall, C. W., E. F. Bradley, D. P. Rogers, J. B. Edson, and G. S. Young, 1996: Bulk parameterization of air–sea fluxes for TOGA COARE. J. Geophys. Res., 101, 3747–3764.

Fairall, C. et al. 2010. Observations to quantify air-sea fluxes and their role in climate variability and predictability, Plenary White Paper in Proceedings of the "OceanObs'09: Sustained Ocean Observations and Information for Society" Conference. ESA Publication WPP-306, Venice, Italy, 21-25 Sept 2009

Fairall, C. W., E. F. Bradley, J. E. Hare, A. A. Grachev, and J. B. Edson, 2003: Bulk parameterization of air–sea fluxes: Updates and verification for the COARE algorithm. J. Climate, 16, 571–591.

Føre, I., J. E. Kristjansson, E. W. Kolstad, T. J. Bracegirdle, Ø. Saetra, and B. Røsting, 2012: A ‘hurricane-like’ polar low fuelled by sensible heat flux: High-resolution numerical simulations, Q. J. R. Meteorol. Soc., 138, 1308–1324, doi:10.1002/qj.1876.

Garratt, J. R., 1977: Review of Drag Coefficients Over Oceans and Continents. Mon. Wea. Rev., 105, 915-929.

Grachev, A. A., C. W. Fairall, J. E. Hare, J. B. Edson, and S. D. Miller, 2003: Wind Stress Vector over Ocean Waves, J. Phys. Oceanogr., 33, 2408–2429.

Grist, J. P. and S. A. Josey, 2003: Inverse Analysis of the SOC Air-Sea Flux Climatology Using Ocean Heat Transport Constraints, Journal of Climate, 16(20), 3274-3295.

Gulev S., et al., 2010: Surface energy and CO2 fluxes in the Global Ocean-Atmosphere-Ice System. Plenary White Paper in Proceedings of the "OceanObs'09: Sustained Ocean Observations and Information for Society" Conference. ESA Publication WPP-306, Venice, Italy, 21-25 Sept 2009.

Gulev, S. K. and K. Belyaev, 2012: Probability Distribution Characteristics for Surface Air–Sea Turbulent Heat Fluxes over the Global Ocean. J. Climate, 25, 184–206, https://doi.org/10.1175/2011JCLI4211.1

Hansen, J., et al., 2005: Earth’s energy imbalance: Confirmation and implications. Science, 308, 1431–1435.

Isemer, H., J. Willebrand, and L. Hasse, 1989: Fine adjustment of large-scale air–sea energy flux parameterizations by direct estimates of ocean heat transport. J. Climate, 2, 1173–1184.

Jackson, D.L., G.A. Wick, and J.J. Bates, 2006: Near-surface retrieval of air temperature and specific humidity using multi-sensor microwave satellite observations. J. Geophys. Res. 111, D10306.

Jin, X., and L. Yu, 2013: Assessing high-resolution analysis of surface heat fluxes in the Gulf Stream region. J. Geophys. Res., Oceans, 118, 5353-5375, doi:10.1002/jgrc.20386.

Jin, X., L. Yu, D. L. Jackson, and G. A. Wick, 2015. An Improved Near-Surface Specific Humidity and Air Temperature Climatology for the SSM/I Satellite Period. J. Atmos. Oceanic Technol., 32, 412–433.

Josey, S. A., E. C. Kent and P. K. Taylor, 1999: New Insights into the Ocean Heat Budget Closure Problem from Analysis of the SOC Air-Sea Flux Climatology. Journal of Climate, 12(9), 2856 - 2880.

Josey, S.A., S. Gulev, and L. Yu, 2013. Exchanges through the ocean surface. In, Siedler, G., Griffies, S., Gould, J. and Church, J. (eds.) Ocean Circulation and Climate: A 21st Century Perspective. 2nd Ed. Oxford, GB, Academic Press, 115-140. (International Geophysics, 103).

Kalnay, E., et al., 1996: The NMC/NCAR 40-year Reanalysis Project. Bull. Amer. Meteor. Soc., 77, 437-471.

Kanamitsu, M, W. Ebisuzaki, J. Woollen, S-K Yang, J .J. Hnilo, M. Fiorino, and G. L. Potter, 2002: NCEP-DOE AMIP-II Reanalysis (R-2),. Bull. Amer. Met. Soc., 83, 1631-1643.

Kato, S., et al., 2013: Surface irradiances consistent with CERES-derived top-of-atmosphere shortwave and longwave irradiances. J. Climate, 26, 2719–2740

Kobayashi, S., et al., 2015: The JRA-55 Reanalysis: General specifications and basic characteristics. J. Meteorol. Soc. Japan, 93, 5-48, doi:10.2151/jmsj.2015-001.

Kubota, M., K. Ichikawa, N. Iwasaka, S. Kizu, M. Konda, and K. Kutsuwada, 2002: Japanese ocean flux data sets with use of remote sensing observations (J-OFURO), J. Oceanogr., 58, 213–215

Landwehr, S., N. O'Sullivan, and B. Ward, 2015: Direct Flux Measurements from Mobile Platforms at Sea: Motion and Airflow Distortion Corrections Revisited. J. Atmos. Oceanic Technol., 32, 1163–1178.

Large, W. G., and S. Pond, 1981: Open ocean momentum flux measurements in moderate to strong winds. J. Phys. Oceanogr., 11, 324–336.

Large, W. G., G. Danabasoglu, S. C. Doney, and J. C. McWilliams, 1997: Sensitivity to surface forcing and boundary layer mixing in a global ocean model: Annual mean climatology. J. Phys. Oceanogr., 27, 2418–2447.

Large, W. G., and S. G. Yeager, 2009: The global climatology of an interannually varying air-sea flux data set. Clim. Dyn., 33, 341–364.

Levitus, S., J. Antonov, T. Boyer, and C. Stephens, 2005: Warming of the world ocean, 1955–2003. Geophys. Res. Lett., 32, L02604, doi:10.1029/2004GL021592.

Liu C., and Coauthors, 2017: Evaluation of satellite and reanalysis-based global net surface energy flux and uncertainty estimates. J. Geophys. Res., Atmospheres, 122(12), 6250–6272.

Liu, W. T., K. B. Katsaros, and J. A. Businger, 1979: Bulk parameterization of air–sea exchanges of heat and water vapor including the molecular constraints at the interface. J. Atmos. Sci., 36, 1722–1735.

Liu, W. T., 1988: Moisture and latent heat flux variabilities in the tropical Pacific derived from satellite data, J. Geophys. Res., 93, 6749–6760.

Loeb, N. G., and co-authors, 2012: Observed changes in top-of-the-atmosphere radiation and upper-ocean heating consistent within uncertainty. Nat Geosci 5(2):110–113. doi: 10.1038/Ngeo1375.

Loeb, N.G., et al., 2018: Clouds and the Earth's Radiant Energy System (CERES) Energy Balanced and Filled (EBAF) Top-of-Atmosphere (TOA) Edition-4.0 Data Product. J. Climate, 31, 895–918,

Louis, J. F., 1979: A Parametric Model of Vertical Eddy Fluxes in the Atmosphere, Bound.-Lay. Meteorol., 17, 187–202.

Miller, M. J., A. C. M. Beljaars, and T. N. Palmer, 1992: The sensitivity of the ECMWF model to the parameterization of evaporation from the tropical oceans. J. Climate, 5, 418–434.

Molod, A., L. Takacs, M. Suarez, and J. Bacmeister, 2015: Development of the GEOS-5 atmospheric general circulation model: evolution from MERRA to MERRA2, Geosci. Model Dev., 8, 1339-1356, doi:10.5194/gmd-8-1339-2015.

Monin, A. S., and A. M. Obukhov, 1954: Basic regularity in turbulent mixing in the surface layer of the atmosphere. Tr. Geofiz. Inst., Akad. Nauk SSSR,24, 163–187.

Newman, M., P. D. Sardeshmukh, and J. W. Bergman, 2000: An assessment of the NCEP, NASA, and ECMWF reanalyses over the tropical west Pacific warm pool. Bull. Am. Meteorol. Soc., 81(1), 41-48.

Paulson, C. A., E. Leavitt, and R. G. Fleagle, 1972: Air-Sea Transfer of Momentum, Heat and Water Determined from Profile Measurements During BOMEX, J. Phys. Oceanogr., 2. 487-497.

Powell, M. D., Vickery, P. J., and Reinhold, T. A., 2003. Reduced drag coefficient for high wind speeds in tropical cyclones, Nature, 422, 279–283.

Prytherch, J., E. C. Kent, S. Fangohr, and D. I. Berry, 2014: A comparison of SSM/I-derived global marine surface-specific humidity datasets. Int. J. Climatol., 35, 2359–2381.

Rienecker, M. M., et al., 2011: MERRA: NASA's Modern-Era Retrospective Analysis for Research and Applications. J. Climate, 24, 3624–3648, doi:10.1175/JCLI-D-11-00015.1

Roberts, J.B., Clayson, C.A., Robertson, F.R., Jackson, D., 2010. Predicting near - surface characteristics from SSM/I using neural networks with a first guess approach. J. Geophys. Res. 115, D19113. http://dx.doi.org/10.1029/2009JD013099.

Rosenfeld, D. and I. M. Lensky, 1998: Satellite-based insights into precipitation formation processes in continental and maritime convective clouds. Bull. Am. Meteorol. Soc., 79, pp. 2457-2476.

Serreze, M. C., A. P. Barrett, A. G. Slater, M. Steele, J. Zhang, and K. E. Trenberth, 2007: The large-scale energy budget of the Arctic, J. Geophys. Res., 112, D11122.

Soloviev, A., R. Lukas, M. Donelan, B. Haus, and I. Ginis, 2014: The air-sea interface and surface stress under tropical cyclones. Sci. Rep., 4, 5306, doi:https://doi.org/10.1038/srep05306.

Trenberth, K. E. and J. M. Caron, 2001: Estimates of meridional atmosphere and ocean heat transports. J. Climate, 14, 3433–3443.

Trenberth, K. E., J. T. Fasullo, M. A. Balmaseda, 2014: Earth's energy imbalance. J Clim 27(9):3129–3144. doi: 10.1175/Jcli-D-13-00294.1

Saha, S., et al., 2010: The NCEP Climate Forecast System Reanalysis. Bull. Amer. Meteor. Soc., 91(8), 1015-1057, doi:10.1175/2010BAMS3001.1

Schlüssel, P., L. Schanz, and G. Englisch, 1995: Retrieval of latent-heat flux and longwave irradiance at the sea-surface from SSM/I and AVHRR measurements, Adv. Space Res., 16, 107–116.

Schulz, J., J. Meywerk, S. Ewald, and P. Schlüssel, 1997: Evaluation of satellite-derived latent heat fluxes. J. Climate, 10, 2782 - 2795.

Simonot, J.-Y. R. and C. Gautier, 1989: Satellite estimates of surface evaporation in the Indian Ocean during the 1979 monsoon. Ocean-Air Interactions 1: 239-256.

Smith, S. D., 1988: Coefficients for sea surface wind stress, heat flux, and wind profiles as a function of wind speed and temperature. J. Geophys. Res., 93, 15 467–15 472.

Stephens, G. L., and co-authors, 2012: An update on earth's energy balance in light of the latest global observations. Nat Geosci 5(10), 691–696.

Valdivieso, et al., 2017: An assessment of air–sea heat fluxes from ocean and coupled reanalyses. Climate Dynamics 49:3, 983-1008.

von Schuckmann, et al. 2016: An im- perative to monitor Earth's energy imbalance, Nature Climate Change, 6, 138–144.

Webster, P.A., R. Lukas, 1992: The Coupled Ocean-Atmosphere Response Experiment. Bull.Am. Met. Soc. , 73 , 1377-1416.

Weller, R. A., E. F. Bradley, R. Lukas, 2004: The interface or air-sea flux component of the TOGA Coupled Ocean-Atmosphere Response Experiment and its impact on subsequent air-sea interaction studies. J. Atmos. Oceanic Tech., 21 ,223-257.

Weller, R., F. Bradley, J. Edson, C. Fairall, I. Brooks, J. Yelland, and W. Pascal, 2008: Sensors for physical fluxes at the sea surface: energy, heat, water, salt. Ocean Sci. Discuss., 5, 327-373.

WCRP, 1989: WOCE Surface Flux Determinations – A strategy for in situ measurements. Working Group on in situ measurements for Fluxes WCRP-23 (WMO/TD No.304), WMO, Geneva.

WGASF, 2000: Intercomparison and validation of ocean-atmosphere energy flux fields—Final report of the Joint WCRP/SCOR Working Group on Air-Sea Fluxes (WGASF). P. K. Taylor, Ed. WCRP-112, WMO/TD-1036, World Climate Research Programme, Geneva. pp 306.

Wild M., D. Folini, C. Schar, N. Loeb, E. G. Dutton, G. König-Langlo, 2013: The global energy balance from a surface perspective. Clim. Dyn., 40(11–12), 3107–3134. doi: 10.1007/S00382-012-1569-8.

Wunsch, C., 2005: The total meridional heat flux and its oceanic and atmospheric partition. J. Climate, 18, 4374–4380.

Yu, L., and R. A. Weller, 2007: Objectively Analyzed air-sea heat Fluexes (OAFlux) for the global ocean, Bull. Am. Meteorol. Soc., 88(5), 527–539.

Yu, L., X. Jin, and R. A. Weller, 2008: Multidecade Global Flux Datasets from the Objectively Analyzed Air-sea Fluxes (OAFlux) Project: Latent and sensible heat fluxes, ocean evaporation, and related surface meteorological variables. Woods Hole Oceanographic Institution, OAFlux Project Technical Report. OA-2008-01, 64pp. Woods Hole. Massachusetts.

Yu, L., et al. 2013:. Towards achieving global closure of ocean heat and freshwater budgets: Recommendations for advancing research in air-sea fluxes through collaborative activities. In Report of the CLIVAR/GSOP/WHOI Workshop on Ocean Syntheses and Surface Flux. Evaluation, Woods Hole, Massachusetts, 27-30 November 2012, WCRP Informal/Series Rep. No. 13/2013, ICPO Informal Rep. 189/13, 42 pp., 2013

Yu, L., and X. Jin, 2014: Insights on the OAFlux ocean surface vector wind analysis merged from scatterometers and passive microwave radiometers (1987 onward). J. Geophys. Res. Oceans, 119, doi:10.1002/2013JC009648.

Yu, L., and X. Jin, 2014: Insights on the OAFlux ocean surface vector wind analysis merged from scatterometers and passive microwave radiometers (1987 onward). J. Geophys. Res. Oceans, 119, 5244-5269.

Yu, L., X. Jin, S. A. Josey, T. Lee, A. Kumar, C. Wen, and X. Yan, 2017: The global ocean water cycle in atmospheric reanalysis, satellite, and ocean salinity. J. Climate, doi: 10.1175/JCLI-D-16-0479.

Yu, L., and X. Jin, 2018: Retrieving near-surface air humidity and temperature using a regime-dependent regression model. Remote Sensing Environ. Revised.

Zeng, X., M. Zhao, and R. E. Dickinson, 1998: Intercomparison of bulk aerodynamic algorithms for the computation of sea surface fluxes using TOGA COARE and TAO data. J. Climate, 11, 2628–2644.

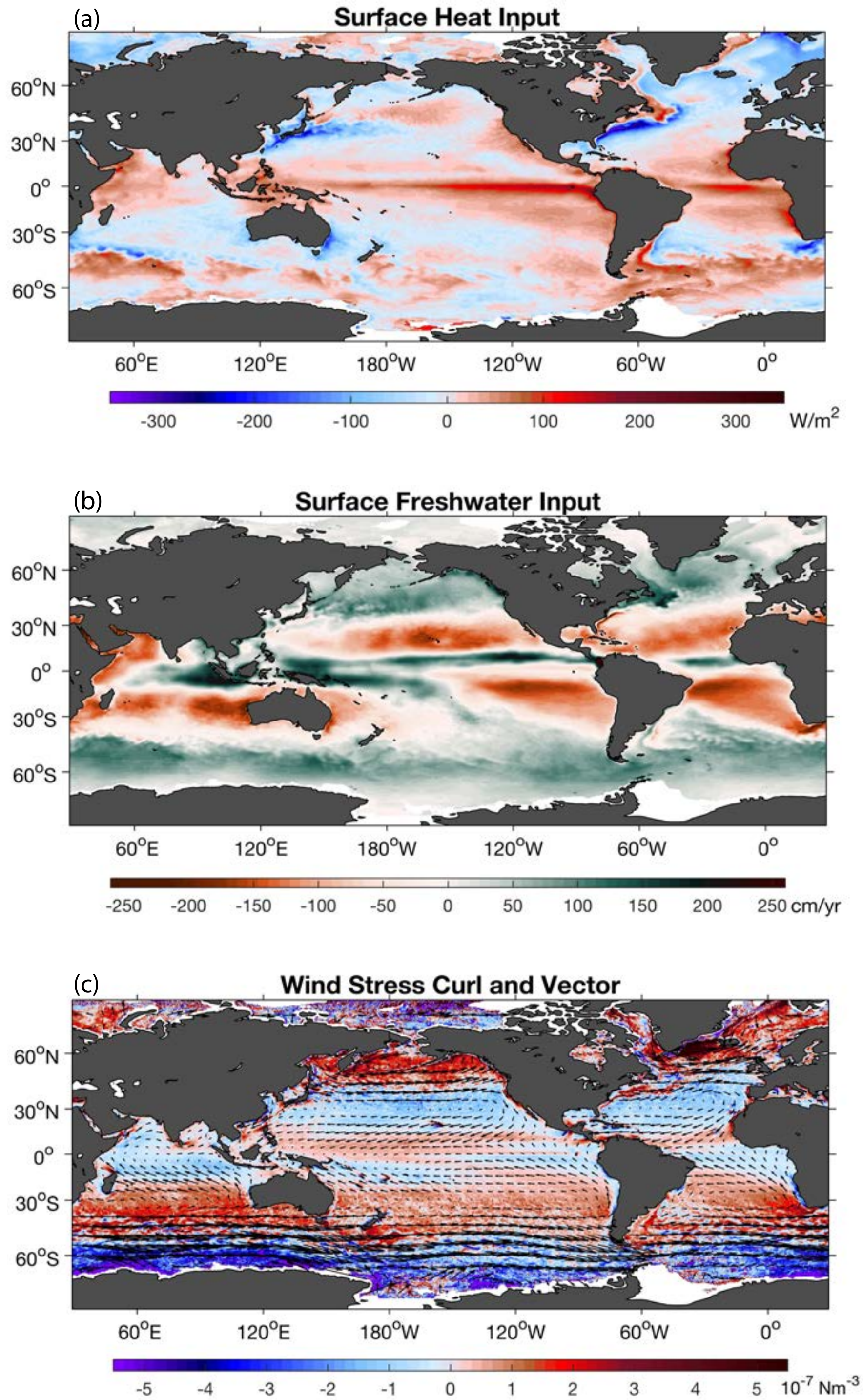

Figure 1. Annual-mean (a) Qnet from CERES+OAFlux-HR4, (b) E-P from OAFlux-HR4 and GPCP, and (b) wind stress vector and wind stress curl (colors) in 2014.

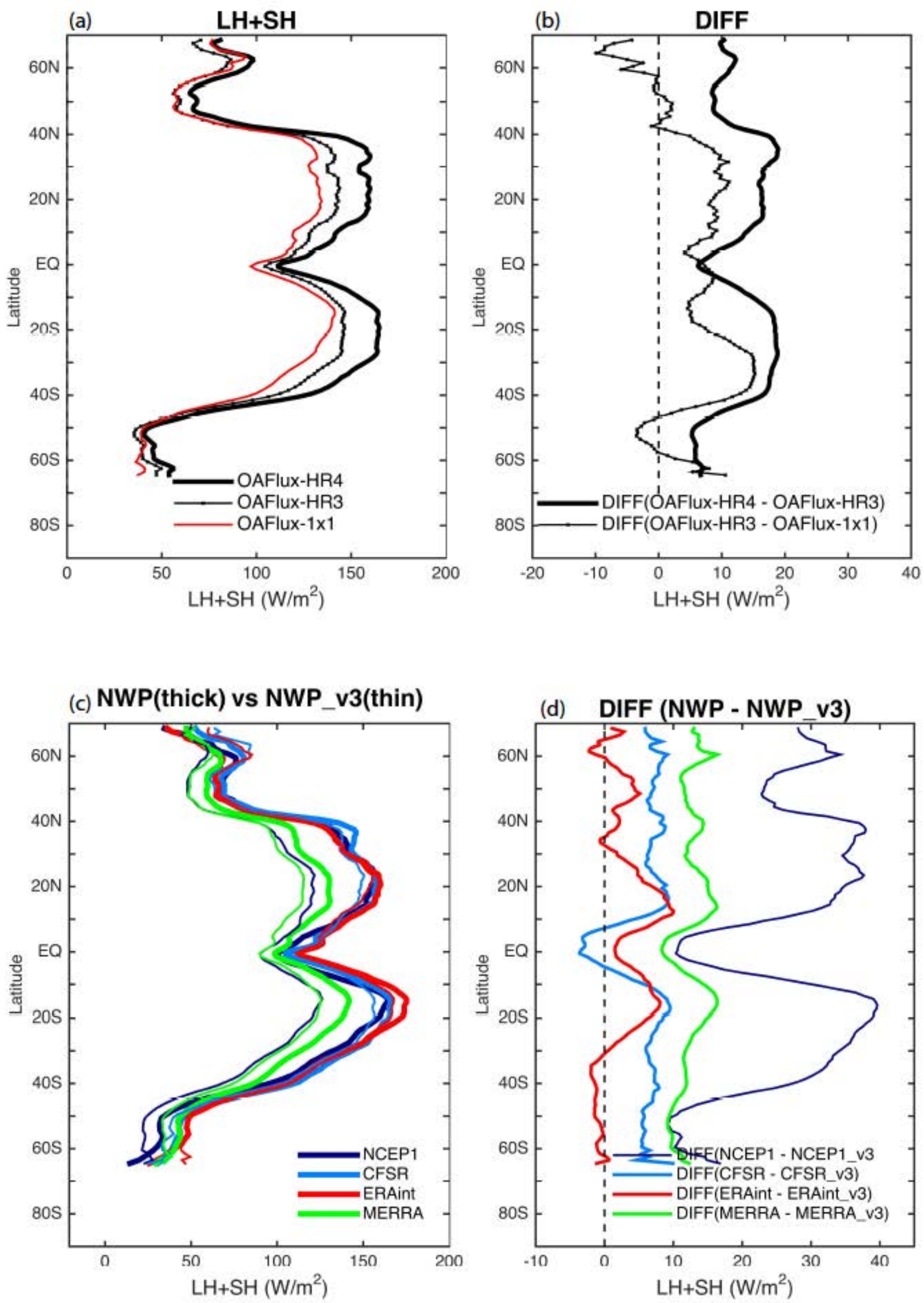

Figure 2. Zonally averaged mean LH+SH in 2014. (a) 3 OAFlux products. (b) Differences between OAFlux-HR4 and HR3 versus between OAFlux-HR3 and 1x1. (c) Original NWP fluxes (thick lines) and recomputed fluxes using NWP variables and COARE v3 algorithm (thin lines). (d) Differences between NWP fluxes and COARE v3 based fluxes.

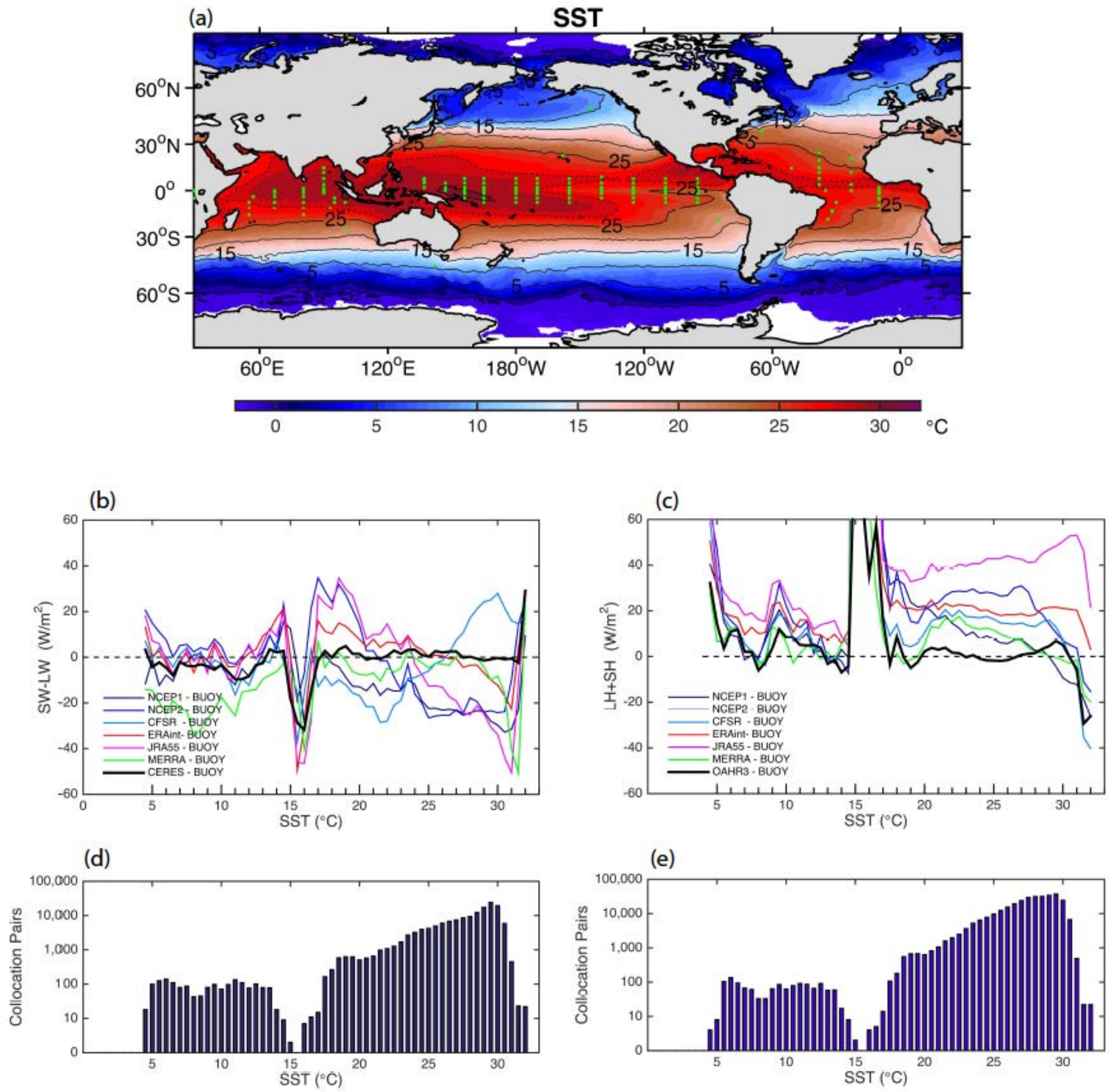

Figure 3. (a) Mean SST field in 2014 superimposed with locations of 126 buoys. (b) Distribution of product-minus-buoy differences in SW-LW with SST. (c) Distribution of product-minus-buoy differences in LH+SH with SST. (d) Number of buoy-product collocation pairs for daily-mean SW-LW. (e) Number of buoy-product collocation pairs for daily-mean LH+SH.

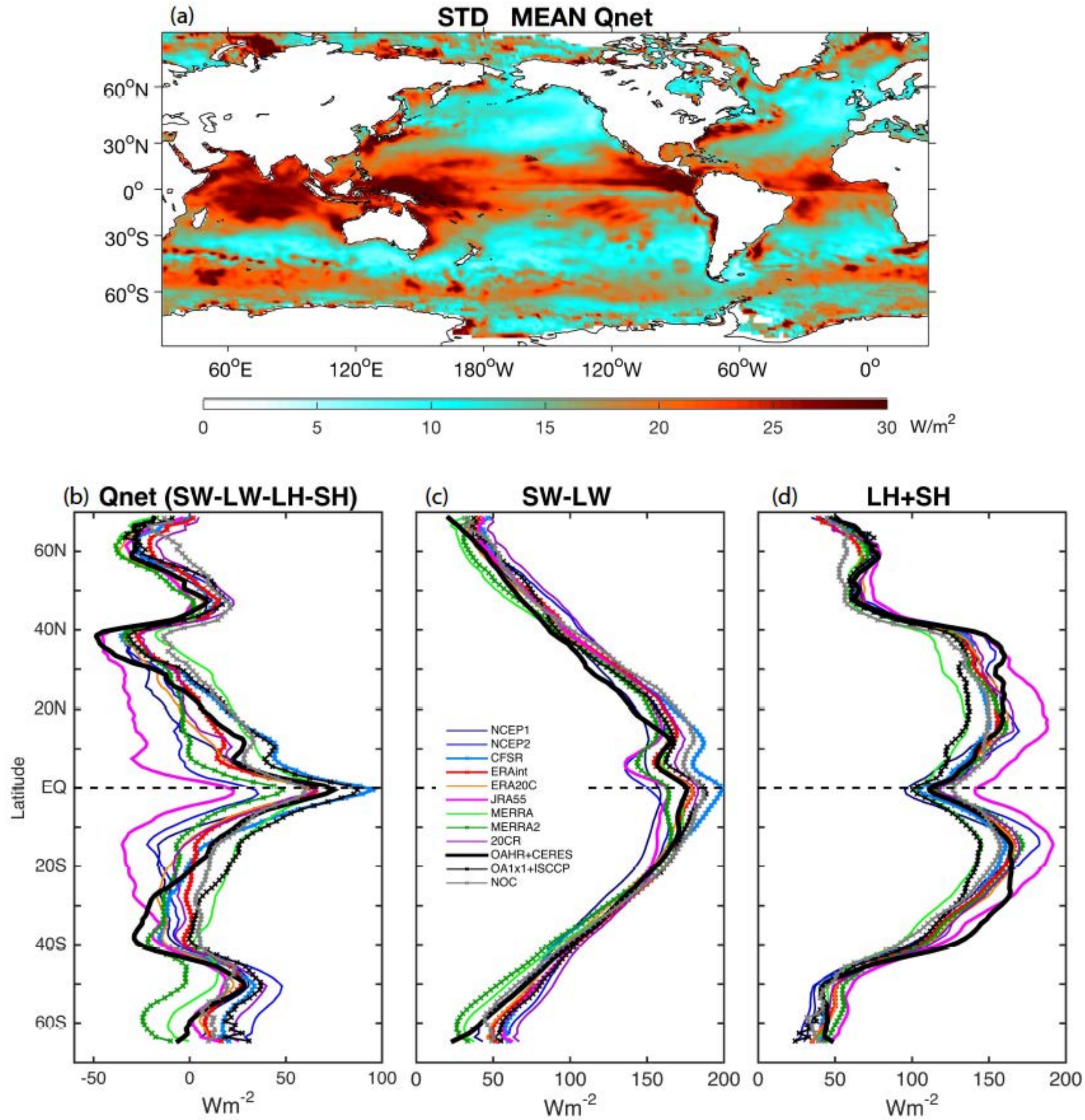

Figure 4. (a) Standard deviations between 12 mean Qnet products. The mean fields are constructed over the 10-year period between 2001 and 2010. Zonal averages of (b) Qnet, (c) SW-LW, and (d) LH+SH.

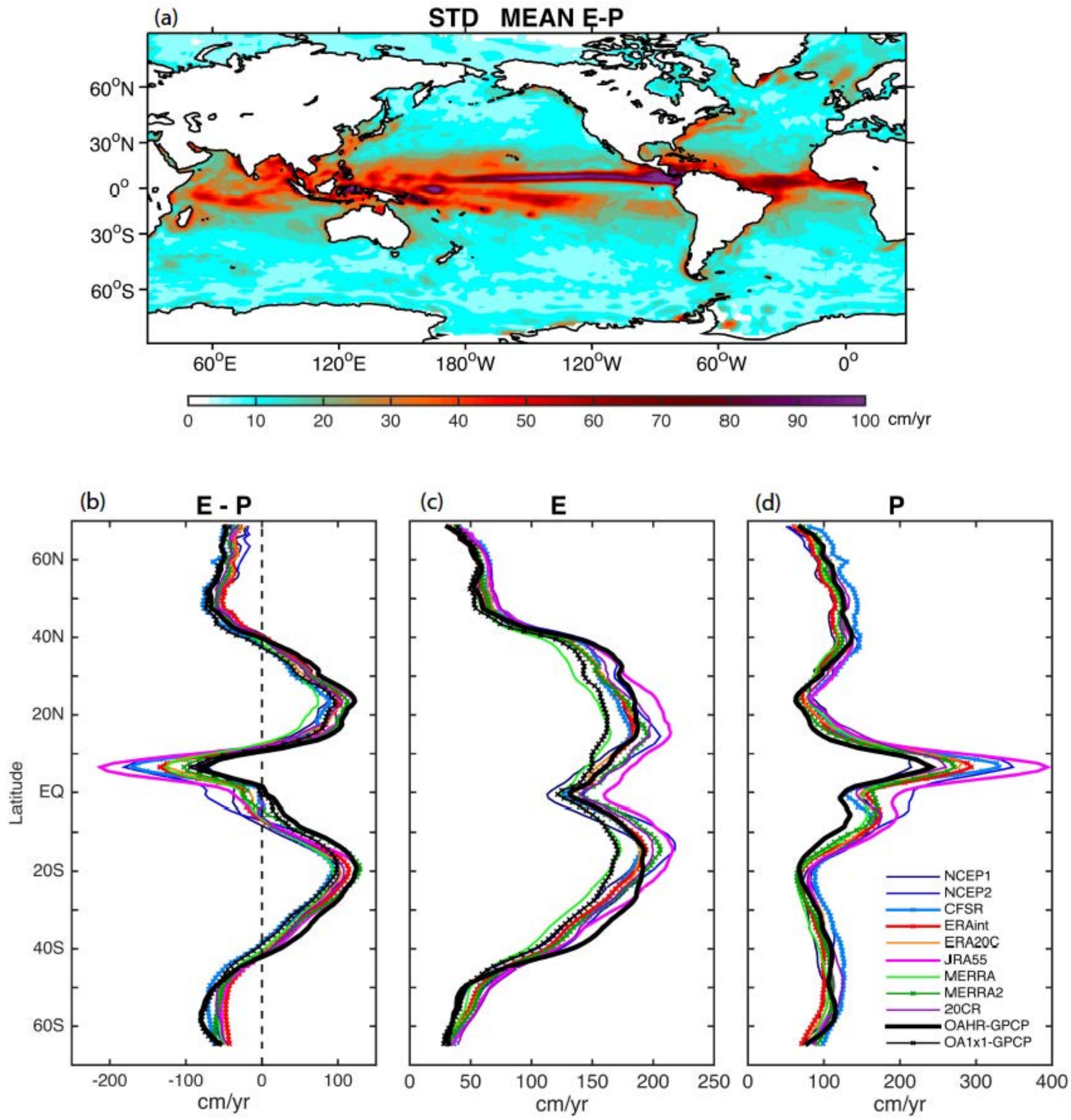

Figure 5. (a) Standard deviations between 11 mean E-P products. The mean fields are constructed over the 10-year period between 2001 and 2010. Zonal averages of (b) E-P, (c) E, and (d) P.

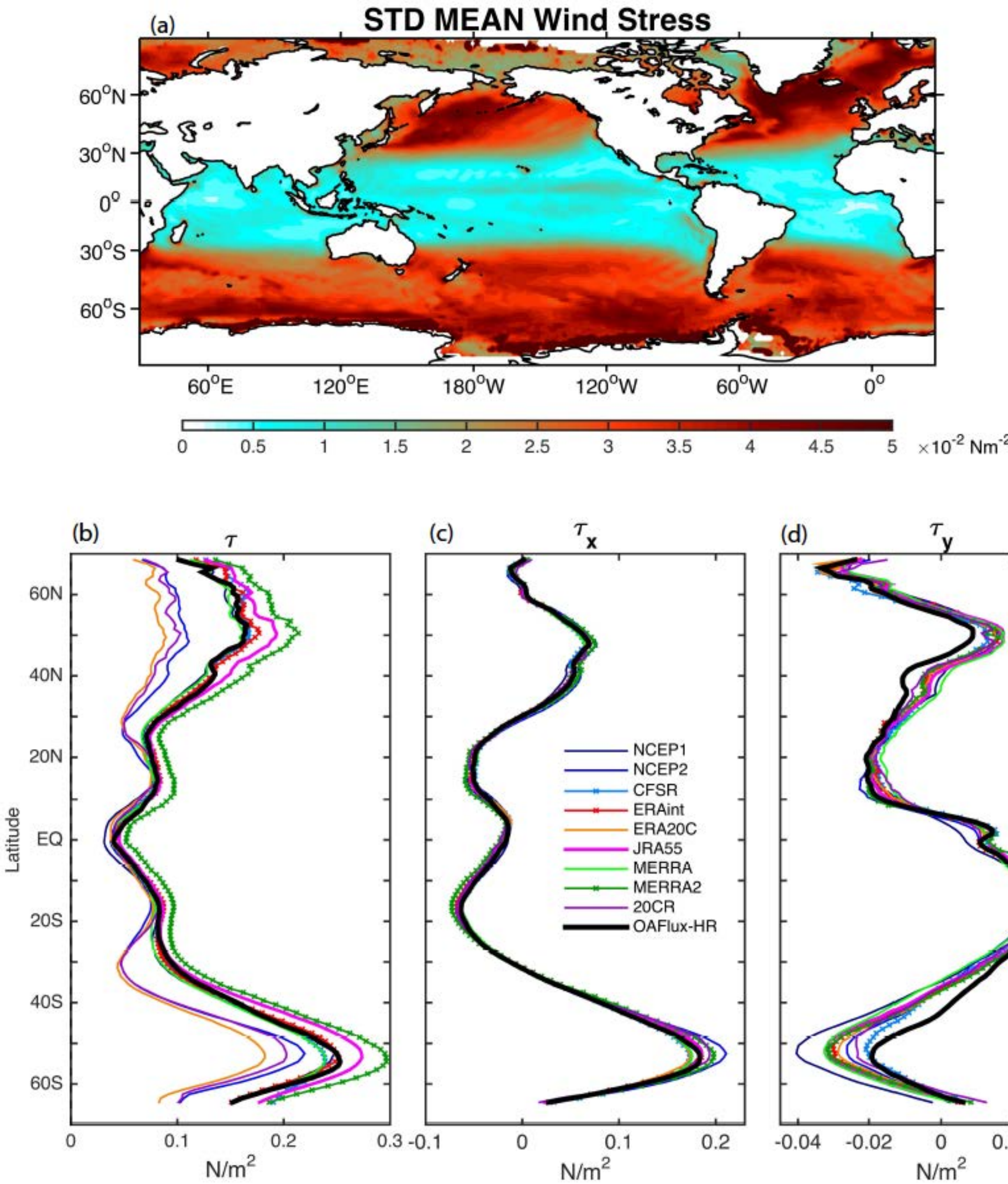

Figure 6. (a) Standard deviations between 10 mean wind stress magnitude products. The mean fields are constructed over the 10-year period between 2001 and 2010. Zonal averages of (b) wind stress magnitude, (c) zonal wind stress, and (d) meridional wind stress.

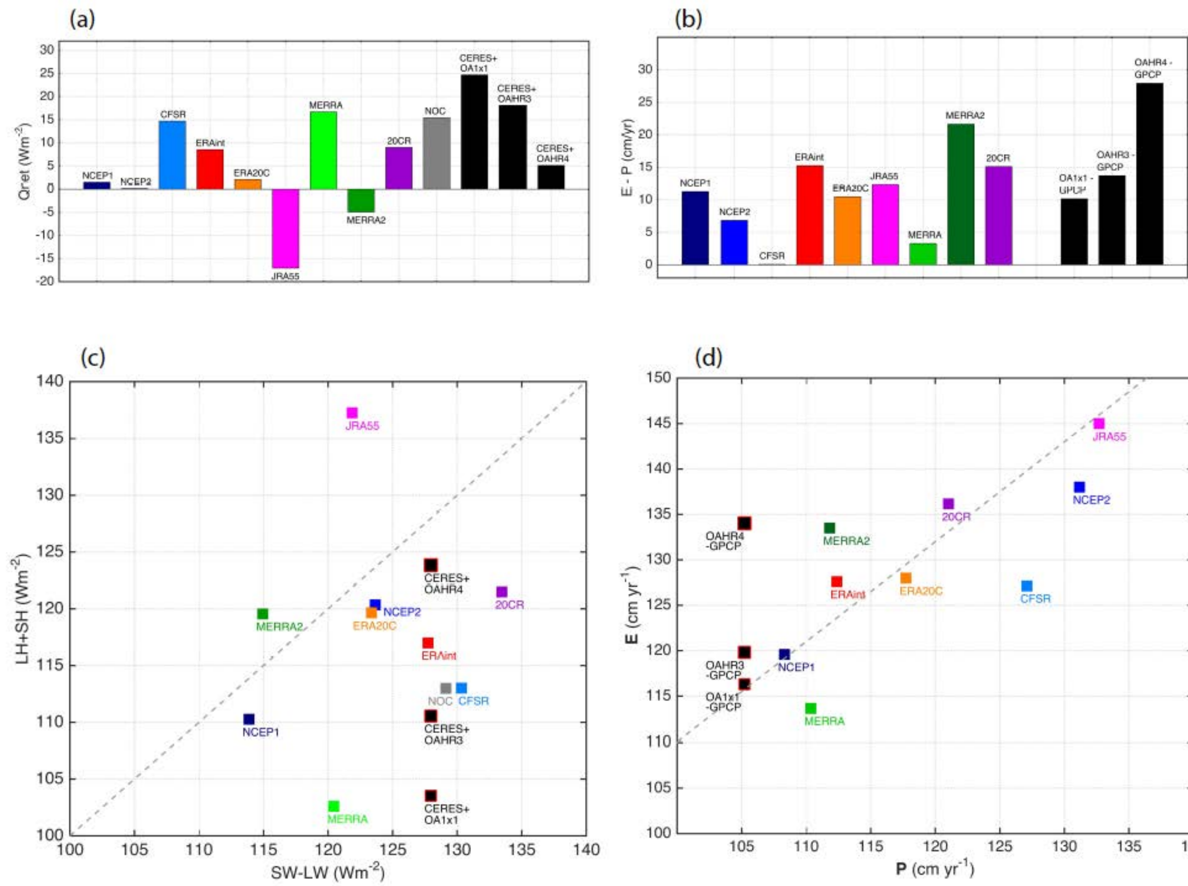

Figure 7. (a) Global-ocean mean energy (Qnet) budget. (b) Global-ocean mean freshwater (E-P) budget. (c) The ratio of mean average of SW-LW to LH+SH. (d) The ratio of mean average of *E* to *P*. The black dash line denotes that the *E/P* ratio equals to 1.10.